

## Experimental investigation of nanofluid shear and longitudinal viscosities

Aaron J. Schmidt,<sup>1,a)</sup> Matteo Chiesa,<sup>1</sup> Darius H. Torchinsky,<sup>2</sup> Jeremy A. Johnson,<sup>3</sup> Avid Boustani,<sup>1</sup> Gareth H. McKinley,<sup>1</sup> Keith A. Nelson,<sup>3</sup> and Gang Chen<sup>1</sup>

<sup>1</sup>Department of Mechanical Engineering, Massachusetts Institute of Technology, Cambridge, Massachusetts 02139, USA

<sup>2</sup>Department of Physics Massachusetts, Institute of Technology, Cambridge, Massachusetts 02139, USA

<sup>3</sup>Department of Chemistry Massachusetts, Institute of Technology, Cambridge, Massachusetts 02139, USA

(Received 25 February 2008; accepted 28 May 2008; published online 20 June 2008)

Dilute nanoparticle suspensions of alumina in decane and isoparaffinic polyalphaolefin (PAO) exhibit thermal conductivity and shear viscosity that are enhanced compared to continuum models that assume well-dispersed particles. An optical technique has been used to measure the longitudinal viscosity of these suspensions at frequencies from 200 to 600 MHz and evaluate an effective hydrodynamic particle size. The measurements indicate that for the decane-based nanofluids the nanoparticles do not form clusters. In the case of PAO nanofluids, the measurements of longitudinal viscosity and the corresponding values of the particle size are consistent with a picture of nonclustered particles in a weakly shear-thinning viscous oligomeric oil. © 2008 American Institute of Physics. [DOI: 10.1063/1.2945799]

Numerous experimental studies have shown that nanoparticle-seeded fluids or “nanofluids” exhibit enhanced thermal conductivity compared to continuum models that assume well-dispersed particles.<sup>1,2</sup> In addition, it has been observed that in some nanofluid systems, the shear viscosity increases more rapidly than predicted by the Einstein model<sup>3</sup> even at concentrations sufficiently small that the systems are truly dilute. The origins of the apparent failure of effective medium theories in both cases have been a subject of considerable debate. One proposed explanation for the enhancement in thermal conductivity and viscosity is that the nanoparticles aggregate, invalidating the assumption of well-dispersed particles.<sup>2,4,5</sup> However, others have argued that aggregation is not an all-inclusive explanation, particularly in stable suspensions at truly dilute volume fractions, and have used models based on Brownian dynamics to explain the data.<sup>6</sup>

In this letter, we present shear and longitudinal viscosity data on two nanofluid systems which exhibit enhanced thermal conductivity: Al<sub>2</sub>O<sub>3</sub> (alumina) nanoparticles in C<sub>10</sub>H<sub>22</sub> (decane) and isoparaffinic polyalphaolefin (PAO). Longitudinal viscosities were measured with an optical technique, impulsive stimulated thermal scattering (ISTS).<sup>7</sup> The longitudinal viscosity of the suspension has a dependence on both volume fraction and particle size,<sup>8,9</sup> allowing us to infer the effective hydrodynamic diameter of the particle in suspension. Our shear viscosity data exhibit an enhancement over the Einstein model, matching the findings of other authors,<sup>5,10,11</sup> and the longitudinal viscosity data indicate that the nanoparticles do not aggregate in these nanofluid systems.

The ISTS measurement is characterized by two distinct time scales: an initial rapid acoustic response, which yields longitudinal viscosity, and a slow thermal decay, which yields thermal conductivity. This approach has the unique advantage compared to other particle-sizing techniques, such as dynamic light scattering and dynamic acoustic scat-

tering,<sup>12</sup> that a single set of measurements simultaneously yields both the thermal conductivity and effective hydrodynamic particle diameter. We chose these nanofluids because hydrocarbon based systems are of potential commercial interest as lubricants with enhanced thermal performance in automotive and other mechanical applications, and because we have previously characterized their thermal conductivity with both ISTS and the standard transient hotwire method.<sup>13</sup> In that work, we found that at a 1% volume fraction of particles, the relative thermal conductivity enhancement of the decane nanofluid was 10.5%, and the enhancement for the PAO nanofluid was 5%, while continuum theory assuming well-dispersed particles predicted a 3% enhancement.

The nanofluids were formulated by mixing alumina nanoparticles (Sigma Aldrich) with a mean particle diameter of 40 nm with two base fluids: 99.9% pure decane and PAO (Synfluid 4cSt, Chevron Phillips). The inset of Fig. 1 shows a transmission electron microscope (TEM) image of the par-

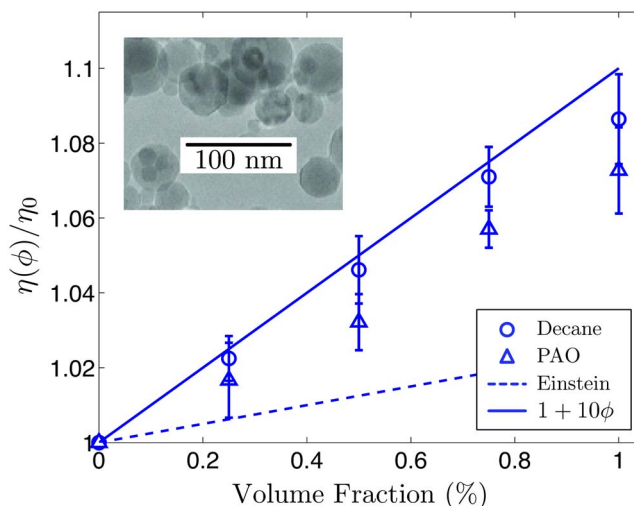


FIG. 1. (Color online) Normalized shear viscosity,  $\eta(\phi)/\eta_0$ , for PAO and decane for volume fractions of alumina from 0.25% to 1%. The inset shows a TEM image of the alumina particles.

<sup>a)</sup>Electronic mail: aarons@mit.edu.

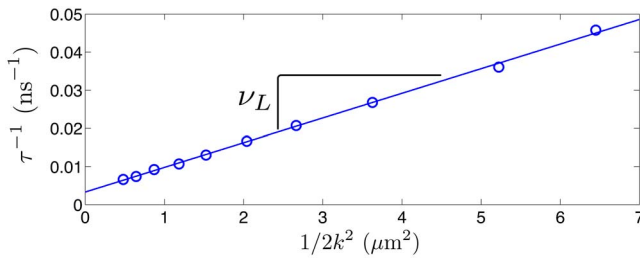


FIG. 2. (Color online) Damping rate for decane with 0.5% alumina at 10 wave vectors plotted against  $1/2k^2$ .

ticles before they are dispersed in the base fluid. The nanofluids were stabilized with 0.25 vol % of sorbitan monolaurate, and the particles were dispersed using an ultrasonic disruptor; a total energy of 5000 J was delivered by a series of 2 s long pulses spaced 5 s apart, with a power density of 2 W/mL. The resulting suspensions did not exhibit sedimentation over several weeks. Shear viscosity measurements were conducted at approximately 22 °C (Fig. 1). The viscosity changed less than 4% over shear rates ranging from 0.33 to 3270  $s^{-1}$ .

In the dilute limit, the Einstein equation<sup>3</sup> predicts that the relative enhancement in the shear viscosity of suspensions of spherical particles is given by  $\eta(\phi)/\eta_0 = 1 + 2.5\phi$ , where  $\eta_0$  and  $\eta(\phi)$  are the viscosity of the base fluid and the nanofluid, respectively. Prasher *et al.*<sup>5</sup> compiled data for alumina nanoparticles in water, ethylene glycol, and polyethylene glycol from their own measurements and those of Wang *et al.*<sup>11</sup> and Das *et al.*<sup>10</sup> The data were well captured for volume fractions of up to 8% by  $\eta(\phi)/\eta_0 = 1 + 10\phi$ ; this result is shown in Fig. 1 for comparison with our own data.

The details of our ISTS apparatus and technique are described elsewhere.<sup>13</sup> Briefly, longitudinal acoustic waves with frequencies from 200 to 600 MHz were created by crossing two 80 ps light pulses in the sample at 8–10 angles ranging from 8.9° to 36.2°. Provided the fluid is Newtonian over the frequency range studied, the measured acoustic decay time  $\tau$  is related to the viscous properties of the medium by  $\tau^{-1} = \frac{1}{2}k^2\nu_L$ ,<sup>14,15</sup> where  $k$  is the wave vector,  $\nu_L = (\frac{4}{3}\eta + \kappa)$  is referred to as the longitudinal viscosity,  $\eta$  is the shear viscosity, and  $\kappa$  is the bulk viscosity. Measurements were carried out on suspensions of alumina in decane and PAO with volume fractions from 0.25% to 1.0%. In all cases, the damping rate  $\tau^{-1}$  was proportional to  $1/2k^2$ . The slope of each curve enables the determination of an effective bulk viscosity  $\nu_L$  for each suspension. A typical result, in this case from decane with 0.5% alumina, is shown in Fig. 2.

When particles are present, the acoustic decay rate includes contributions from the base fluid and the particles:  $\tau^{-1} = \frac{1}{2}k^2\nu_{L,0} + \tau_{\text{part}}^{-1}$ . The first term on the right hand side accounts for the longitudinal viscosity of the base fluid and is found by measuring the base fluid alone. The second term accounts for the additional attenuation due to the particles. In our case, the acoustic decay time is sufficiently fast that thermal decay can be neglected for time scales on the order of 100 ns.<sup>13,15</sup> The particle size ( $\sim 40$  nm) is also much smaller than the acoustic wavelength so we use a continuum approach developed by Harker and Temple (HT).<sup>8</sup> The decay rate due to particles is given by  $\tau_{\text{part}}^{-1} = c_0 \times \text{Im}\{q\}$ , where  $c_0$  is the isentropic sound speed and  $q$  is the complex wave vector given by

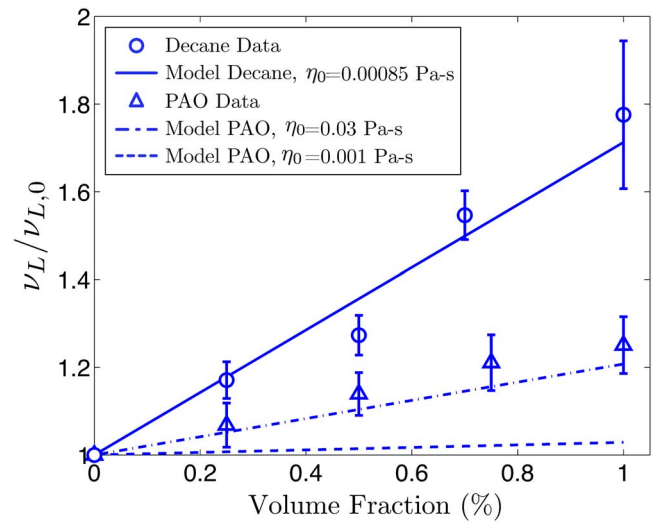


FIG. 3. (Color online) Effective longitudinal viscosity for alumina volume fractions from 0.25% to 1.0%. The Harker–Temple (HT) model matches well for the decane system, but underpredicts for the PAO system when the value of shear viscosity measured at low shear rates,  $\eta_0 = 0.03$  Pa·s, is used. Agreement improves if a lower value for the shear viscosity is assumed to be relevant over the frequency range of the experiment.

$$q^2 = \omega^2[(1 - \phi)\beta] \frac{\rho_f[\rho_s(1 - \phi + \phi S) + \rho_f S(1 - \phi)]}{\rho_s(1 - \phi)^2 + \rho_f[S + \phi(1 - \phi)]}. \quad (1)$$

Here,  $\phi$  is the volume fraction,  $\omega$  is the angular frequency of the wave,  $\beta$  is the compressibility of the fluid,  $\rho_s$  and  $\rho_f$  are the densities of the solid and fluid, respectively, and  $S$  is

$$\frac{1}{2} \left( \frac{1 + 2\phi}{1 - \phi} + \frac{9\delta}{4a} \right) + i \frac{9}{4} \left( \frac{\delta}{a} + \frac{\delta^2}{a^2} \right), \quad (2)$$

where  $a$  is the particle radius,  $\delta = \sqrt{2\eta_0/\omega\rho_f}$  is the viscous penetration depth, and  $\eta_0$  is the shear viscosity of the base fluid.

The total decay rate was computed over the range of wave vectors for our data at each concentration point (Fig. 3). The particle diameter,  $2a$ , was taken as 40 nm determined from TEM images. For these frequencies, the solution damping rate exhibited a Newtonian  $1/2k^2$  dependence and the slope was taken as the effective bulk viscosity of the suspension.

Using the measured shear viscosity, the HT model matches the decane longitudinal viscosity data, but underpredicts attenuation for the PAO suspensions. This discrepancy could be due to clustering or to a reduction in the shear viscosity of PAO at high frequencies. We suspect the latter because of measurements on PAO without particles. For the base fluid, the bulk viscosity  $\kappa$  can be directly deduced from the measured longitudinal and shear viscosities:  $\kappa = \nu_{L,0} - \frac{4}{3}\eta_0$ . In our experiments,  $\nu_{L,0}$  was measured at high frequency while  $\eta_0$  was measured for shear rates from 4 to 700  $s^{-1}$ . For pure decane, this yields  $\kappa = 2.54 \times 10^{-3}$  Pa·s, in good agreement with a literature value.<sup>16</sup> However, for pure PAO, the same operation yields a negative value for bulk viscosity, indicating that the steady shear viscosity must be significantly higher than the shear viscosity at 200–600 MHz. Compared with decane, which is composed of a single hydrocarbon, PAO is a complex mixture of many long-chain hydrocarbons and thus can be expected to have more complex visco-elastic behavior. This idea is further

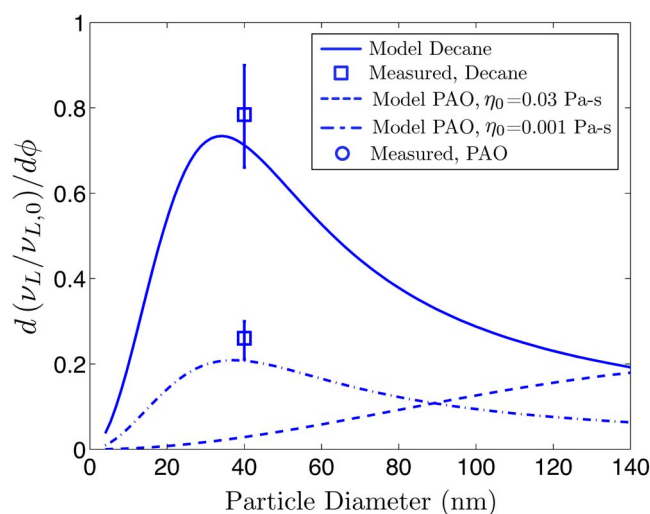


FIG. 4. (Color online) Rate of increase in normalized longitudinal viscosity with vol % particles, plotted as a function of particle diameter. The measured longitudinal viscosity enhancement for each fluid is indicated at 40 nm, the value observed via TEM.

supported by noting that if a lower value of shear viscosity is inserted into the HT model, the result more closely matches the data. The predicted result for PAO using a shear viscosity  $\eta_0$  of 0.001 Pa s is shown in Fig. 3 for reference.

By varying the particle radius in Eq. (1), we can replot the longitudinal viscosity results as a function of particle size (Fig. 4) and deduce the effective hydrodynamic diameter in suspension. For decane, the predicted increase is close to the measured increase using the TEM-observed diameter of  $\sim 40$  nm. Even more interesting is the fact that the function has a strong maximum close to this value, implying that the measured increase in longitudinal viscosity constrains the particle diameter to be in the neighborhood of 40 nm. As in Fig. 3, the fit of the model for the PAO data is poor using the measured zero-shear rate viscosity but improves if a lower value of  $\eta_0$  is used.

For the decane-based nanofluid, Fig. 4 implies that the nanoparticles are not clustering. In the case of PAO, the conclusion is not as clear. Figure 4 shows that either a particle size on the order of 140 nm, or a greatly decreased shear viscosity of the base fluid at high frequency could reproduce the observed result. However, as we discussed above, the measured values of  $\eta_0$  and  $\nu_{L,0}$  would imply a bulk viscosity  $\kappa < 0$  if the fluid were simply a Newtonian fluid with constant viscosity. This implies that there must be some reduction in shear viscosity over the measured dc value. We do not

know exactly what the reduction is, so it is not possible to infer with certainty the effective particle size from the model.

Alumina nanoparticles in decane and in PAO exhibit enhanced thermal conductivity and shear viscosity over classical continuum models that assume well-dispersed particles. The measurements of longitudinal viscosity presented here for decane-based nanofluids yield self-consistent data for nonclustered particles dispersed in a Newtonian solvent of constant viscosity. When combined with the fact that the suspensions are extremely dilute and show no signs of sedimentation, these results indicate that aggregation may not be responsible for the disagreement between effective medium models and the data in all nanofluid systems, and that models based on Brownian dynamics<sup>6</sup> or other nanoscale phenomena should be considered. For the PAO-based nanofluid, the response is more complex and further study of the frequency-dependent viscous response in the oligomeric suspending oil is still required.

We would like to thank Professor Sarit Das for his helpful discussions. This work was partially supported by the Norwegian Research Council, the Ford-MIT alliance, NSF grants CHE-0616939 and DMR-0414895, and a NSF Graduate Research Fellowship for A. Schmidt.

- <sup>1</sup>S. Das, S. Choi, and H. Patel, *Heat Transfer Eng.* **27**, 3 (2006).
- <sup>2</sup>P. Koblinski, R. Prasher, and J. Eapen, *J. Nanopart. Res.* (unpublished).
- <sup>3</sup>A. Einstein, *Ann. Phys.* **34**, 591 (1911).
- <sup>4</sup>R. Prasher, P. E. Phelan, and P. Bhattacharya, *Nano Lett.* **6**, 1529 (2006).
- <sup>5</sup>R. Prasher, D. Song, J. Wang, and P. Phelan, *Appl. Phys. Lett.* **89**, 133108 (2006).
- <sup>6</sup>P. Bhattacharya, S. K. Saha, A. Yadav, P. E. Phelan, and R. S. Prasher, *J. Appl. Phys.* **95**, 6492 (2004).
- <sup>7</sup>J. A. Rogers, A. A. Maznev, M. J. Banet, and K. A. Nelson, *Annu. Rev. Mater. Sci.* **30**, 117 (2000).
- <sup>8</sup>A. H. Harker and J. A. G. Temple, *J. Phys. D: Appl. Phys.* **21**, 1576 (1988).
- <sup>9</sup>M. L. Mather, R. E. Challis, M. J. W. Povey, and A. K. Holmes, *Rep. Prog. Phys.* **68**, 1541 (2005).
- <sup>10</sup>S. K. Das, N. Putra, and W. Roetzel, *Int. J. Heat Mass Transfer* **46**, 851 (2003).
- <sup>11</sup>S. U. S. Choi, X. W. Wang, and X. F. Xu, *J. Thermophys. Heat Transfer* **13**, 474 (1999).
- <sup>12</sup>M. L. Cowan, J. H. Page, and D. A. Weitz, *Phys. Rev. Lett.* **85**, 453 (2000).
- <sup>13</sup>A. J. Schmidt, M. Chiesa, D. H. Torchinsky, J. A. Johnson, K. A. Nelson, and G. Chen, *J. Appl. Phys.* **103**, 083529 (2008).
- <sup>14</sup>J. D. Walecka and A. L. Fetter, *Theoretical Mechanics of Particles and Continua* (McGraw-Hill, New York, 1980).
- <sup>15</sup>Y. Yang and K. A. Nelson, *J. Chem. Phys.* **103**, 7722 (1995).
- <sup>16</sup>M. G. Sceats and J. M. Dawes, *J. Chem. Phys.* **83**, 1298 (1985).